SAND2016-7087PE

Frequency Band Interference for the Attenuation of Combustion Noise in a DI Diesel Engine

Stephen Busch
Sandia National Laboratories

Acknowledgments:

Gurpreet Singh, Leo Breton
DOE EERE, Office of Vehicle Technologies
Financial support

Alok Warey, Francesco Pesce, Richard Peterson
General Motors Company
Technical input

ACEC Meeting: July 21, 2016

Motivation: close-coupled pilot injections can significantly reduce combustion noise

- Combustion noise is computed from cylinder pressure for part-load, conventional operation
  - Vary pilot-main dwell with constant pilot mass, load, and CA50
- Adding a pilot reduces noise, but a further reduction is possible at a specific dwell
- **We want to understand what is responsible for this additional combustion noise reduction**

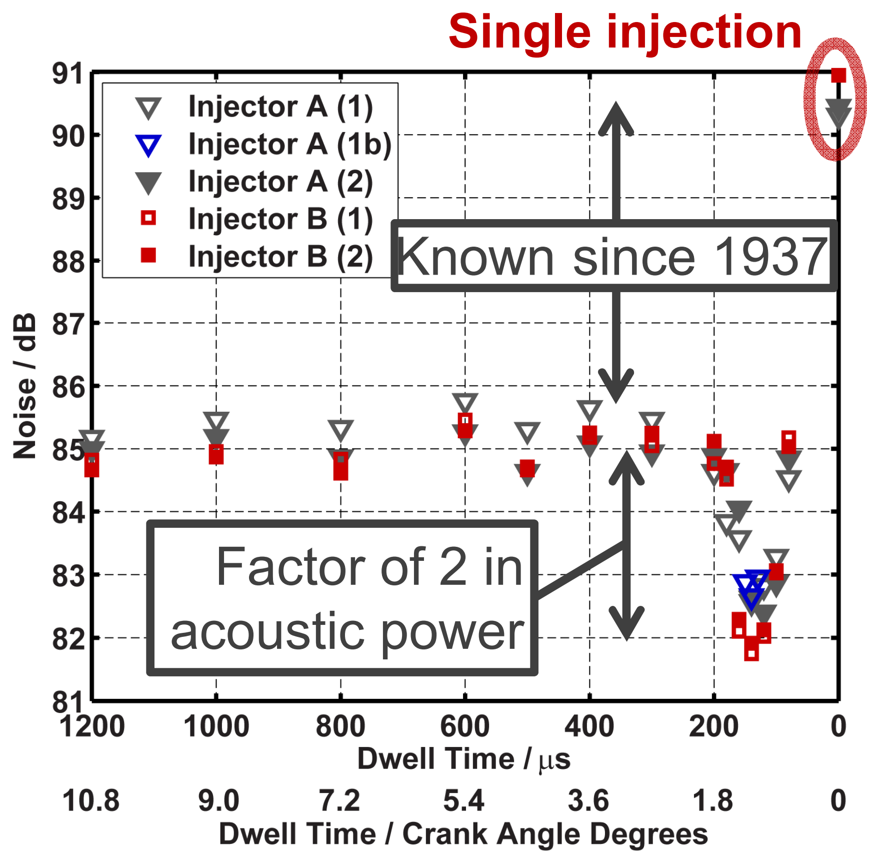

Reduction of noise by pilot injections reported in:
Jâfar, D., *Pilot Injection*, in *Engineering Magazine*. 1937: London.

Combustion noise calculated according to:
Shahlari, A., Hocking, C., Kurtz, E., and Ghandhi, J., "Comparison of Compression Ignition Engine Noise Metrics in Low-Temperature Combustion Regimes," SAE Int. J. Engines 6(1):541-552, 2013, doi:10.4271/2013-01-1659.

Outline

- Experiments
  - Fuel injector dynamics
  - Main injection rate shaping – responsible for the noise reduction?
- Analysis: zero-dimensional thermodynamic model
  - Understanding the combustion noise reduction mechanism
  - Parametric studies
- Summary / Conclusions

Experiments: small-bore Diesel engine

- Thermodynamic – metal piston, skip-fired operation
  - Measure cylinder pressure
    - AHRR
    - Combustion noise [14]
- Optical – fused silica piston, motored operation (N_2)
  - High pulse rate, high intensity LED
  - High speed CMOS camera
    - Liquid fuel imaging
    - 120,000 fps (0.075 CAD at 1500 r/min)
    - Image size: 256 x 256 pixels
    - Automated image distortion correction routine

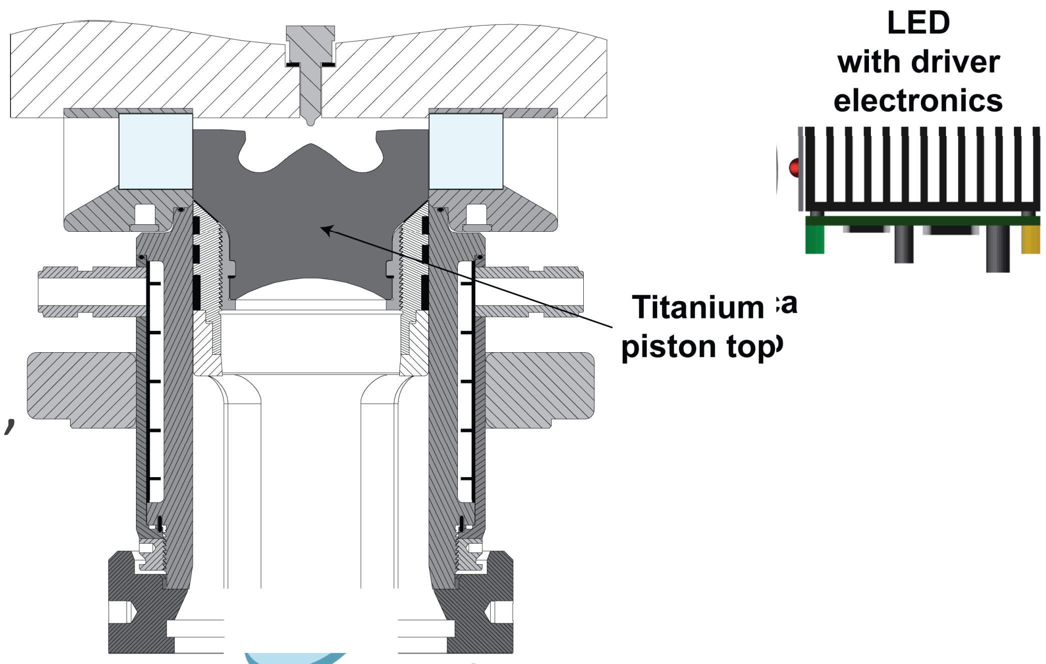

Sample raw image

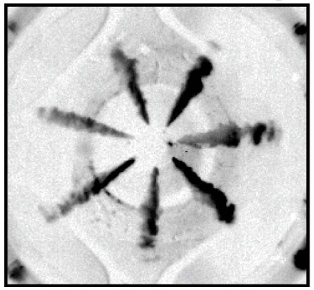

Combustion noise calculated according to:

[14] Shahlari, A., Hocking, C., Kurtz, E., and Ghandhi, J., "Comparison of Compression Ignition Engine Noise Metrics in Low-Temperature Combustion Regimes," SAE Int. J. Engines 6(1):541-552, 2013, doi:10.4271/2013-01-1659.

Experiments: injection rate measurements with the Moehwald HDA

- Same fuel injection hardware as used in engine testing
- Same injection schedules as used in engine testing
- Chamber pressure corresponds to cylinder pressure at start of injection
- Measurement of chamber pressure and speed of sound of fuel in chamber
  - Fuel density and compressibility effects taken into account
- Derived fuel injection rates for each injection schedule

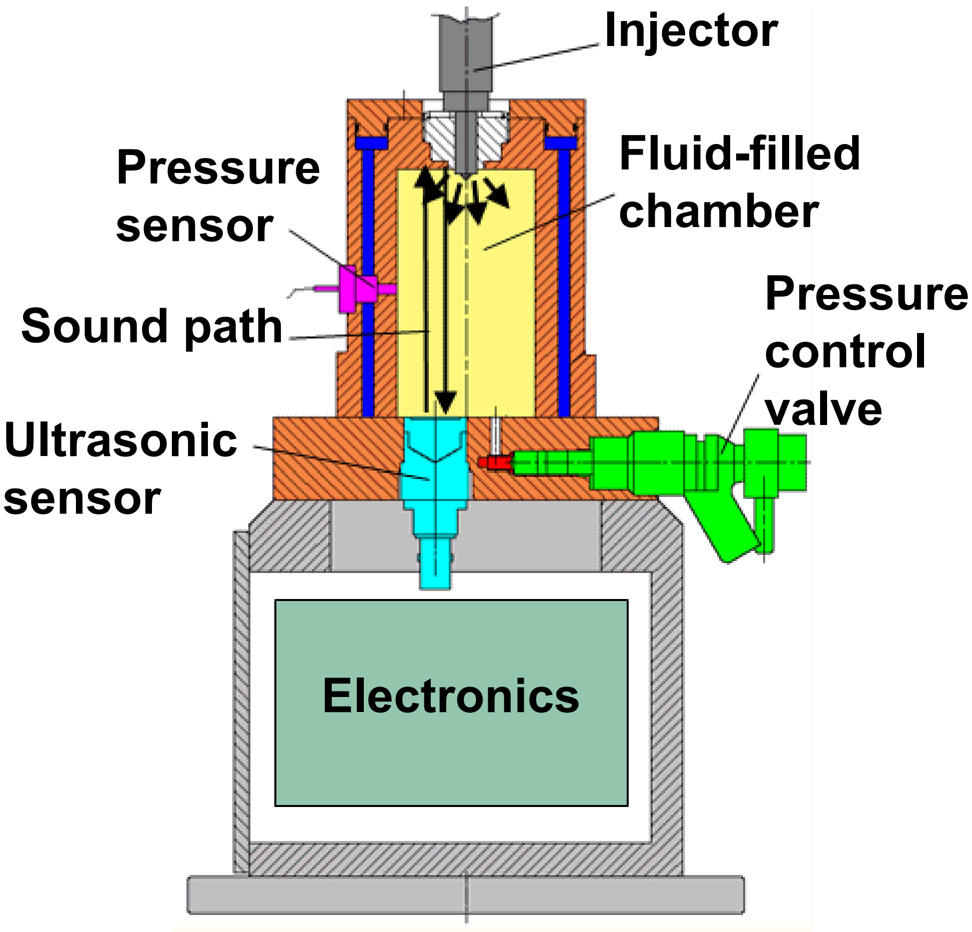

Experiments: operating conditions

- Operating point:
  - 1500 rpm
  - Pilot mass: 1.5 mg/str
  - IMEPg: 9 bar
    - Adjust ET_{main} to maintain load
  - $P_{rail:}$ 800 bar
  - CA50: 13 CAD ATDC
  - Fuel: DPRF58 (58 vol% HMN, 42 vol% n-hexadecane)
- Vary energizing dwell between pilot and main injection
  - 1200 – 80 µs (10.8 CAD – 0.7 CAD)

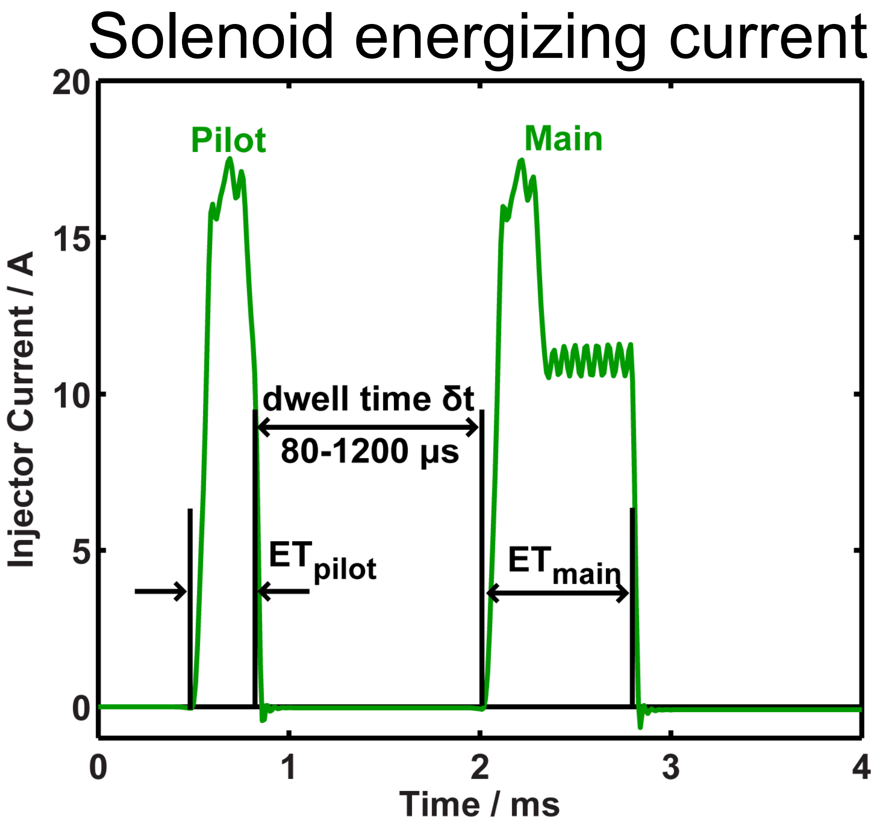

Experimental results: measured injection rates

- Two injection events even for shortest dwells
- Changing dwell changes main injection rate shape
  - Dwell 1200 µs: main injection rate close to single injection rate
  - Dwell 80 µs: steepest injection rate increase
  - Dwell 140 µs: steep at first, less steep thereafter
- Does this rate shaping take place in the engine in this manner?

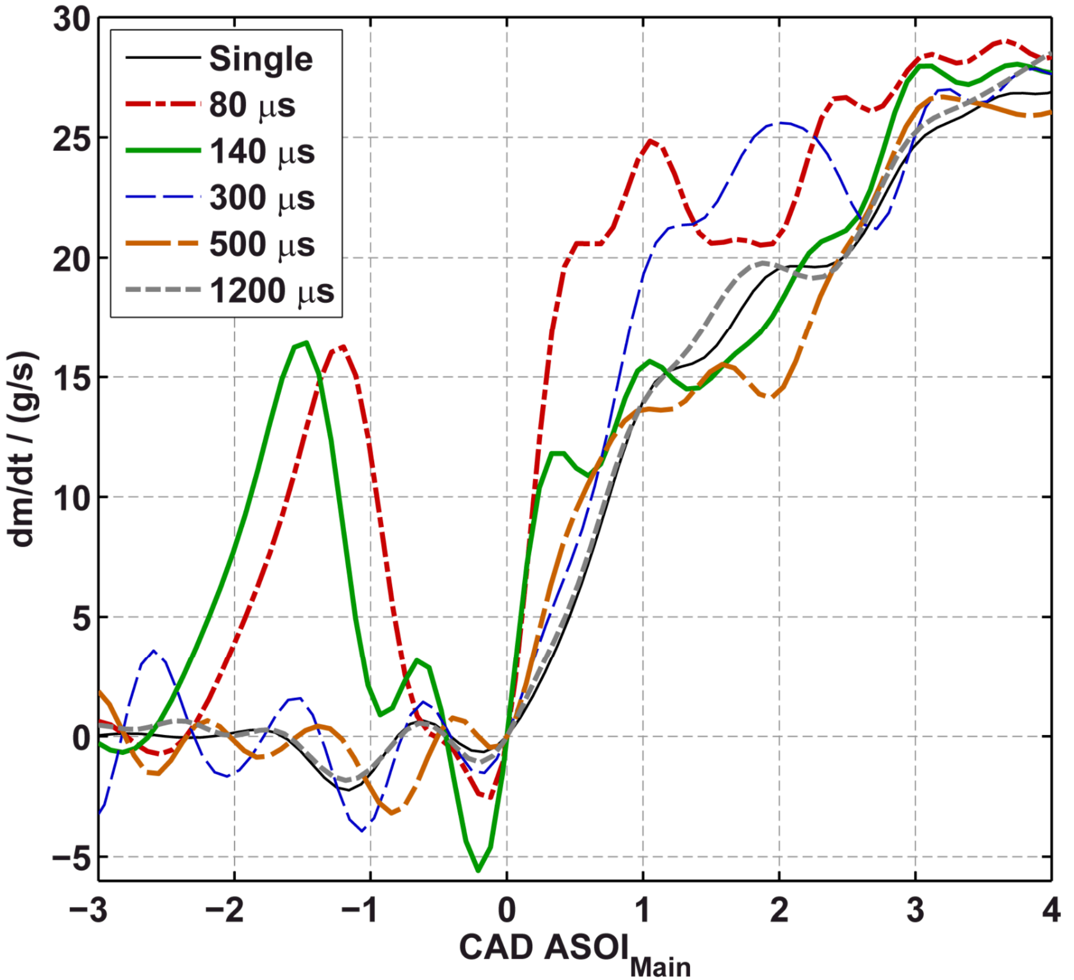

Automated image distortion correction with ray tracing

- Image distortion depends very strongly on the object's proximity to the piston
  - Particularly noticeable near pip
- De-warping to match a flat target image is not viable for imaging of fuel jets
  - Correction for one horizontal plane does not properly de-warp information from other planes
- De-warping performed along injector jet axis
  - Assume information comes only from this conical region of space
  - Final image resolution corresponds to 8 pixels per mm along jet axes

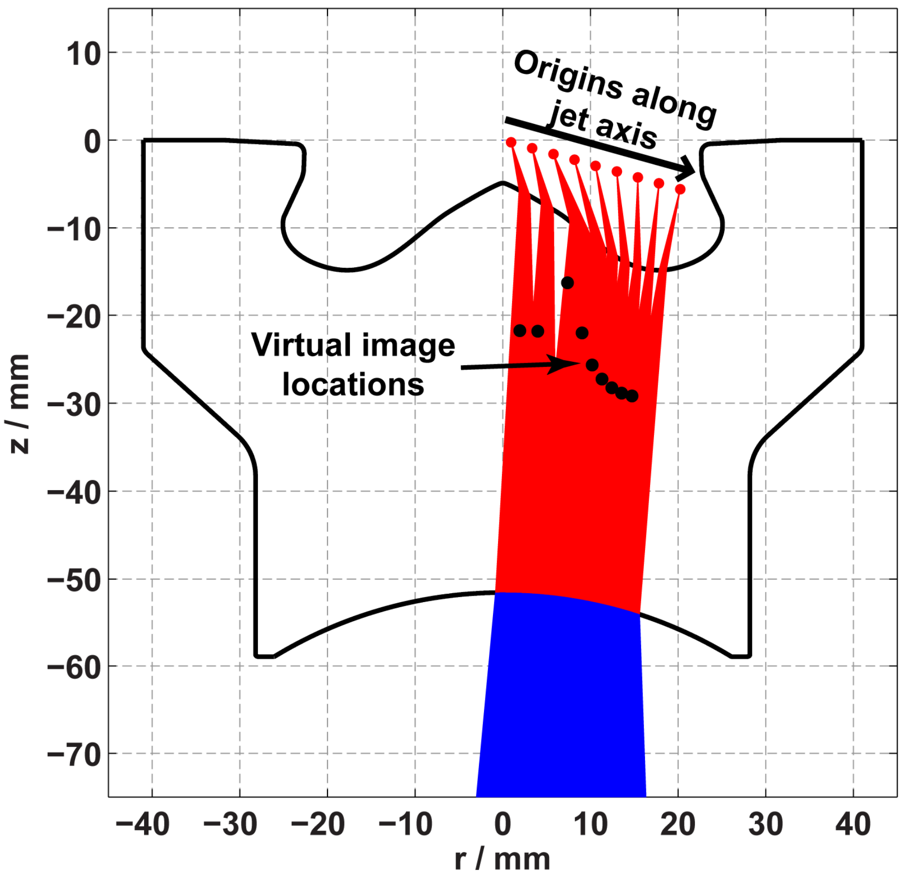

Fuel injection image processing

- Image distortion correction along jet axes
- Background modeling and subtraction with approx. median method
- Quantitative data can be extracted from images
  - Penetration lengths
  - Penetration rates
- Do trends in initial liquid penetration rates correspond to trends in injection rates?

Single cycle

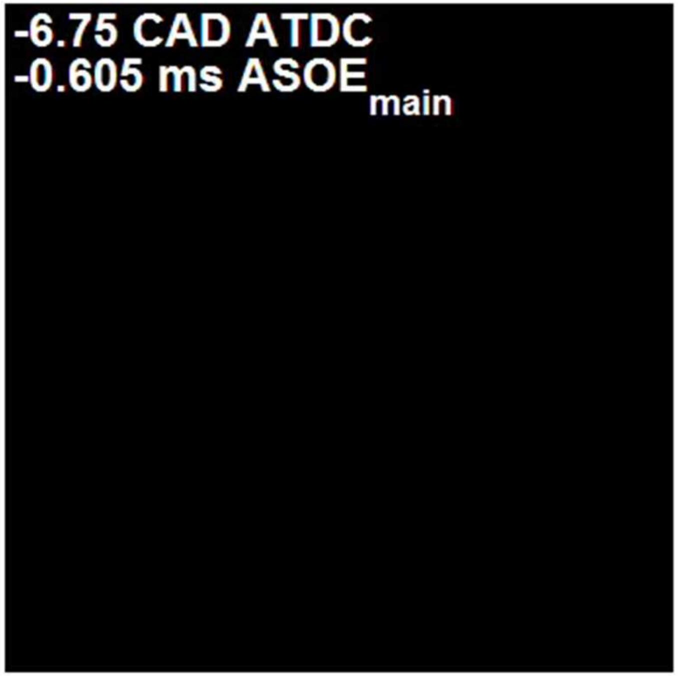

Dwell 300 μs; gamma = 0.7; 0-1024 counts

Optically determined penetration rates correlate with injection rate data

- Injection rate shapes synchronized via solenoid current
- Penetration rate data averaged over all jets
  - Negative values not shown
- Trends in penetration rate seem to agree with rate shape data
  - Phasing of main injection ramp-up
  - Slowest penetration rates for a dwell of 140 µs
  - Relative magnitudes of maximum main injection penetration rate
- Rate shaping does seem to be occurring in the engine
- Can this behavior explain the combustion noise trend?

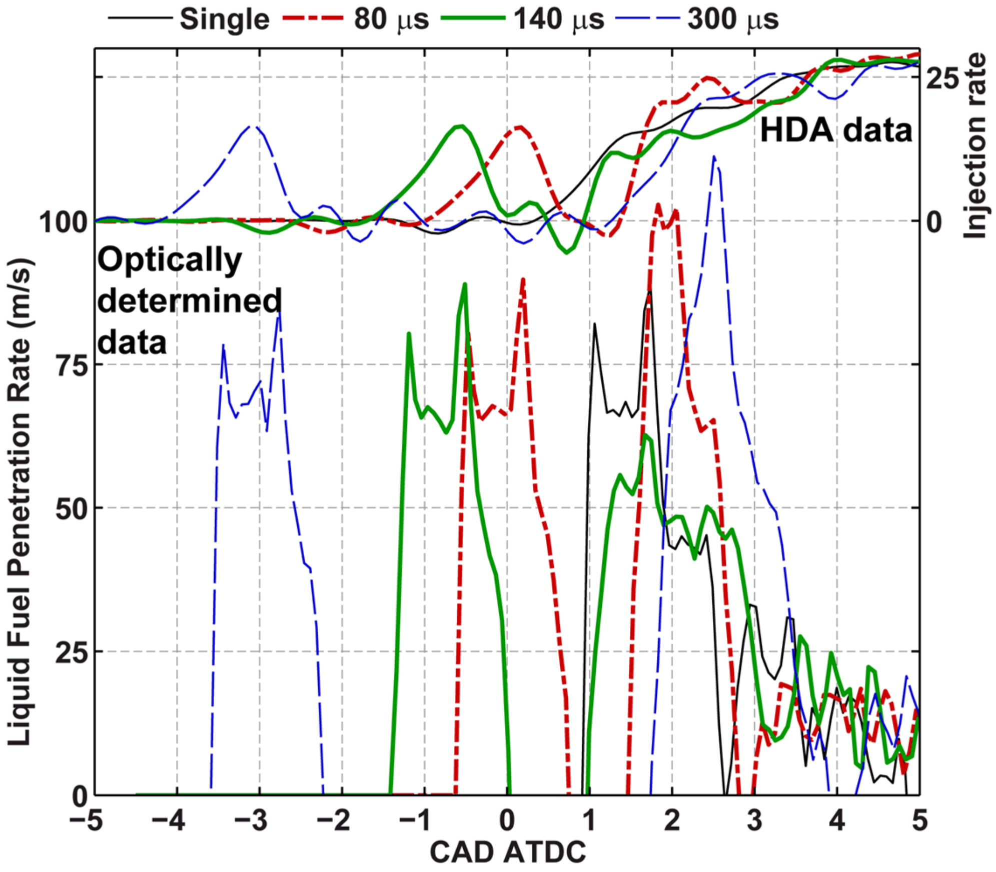

Can main injection rate shaping influence combustion noise?

- Comparison: dwell times of 80 and 1200 μs
  - Largest difference in main injection rate shapes
  - Slight difference in combustion noise
  - Significant differences in premixed combustion behavior
  - Pilot and main AHRR appear to have merged…

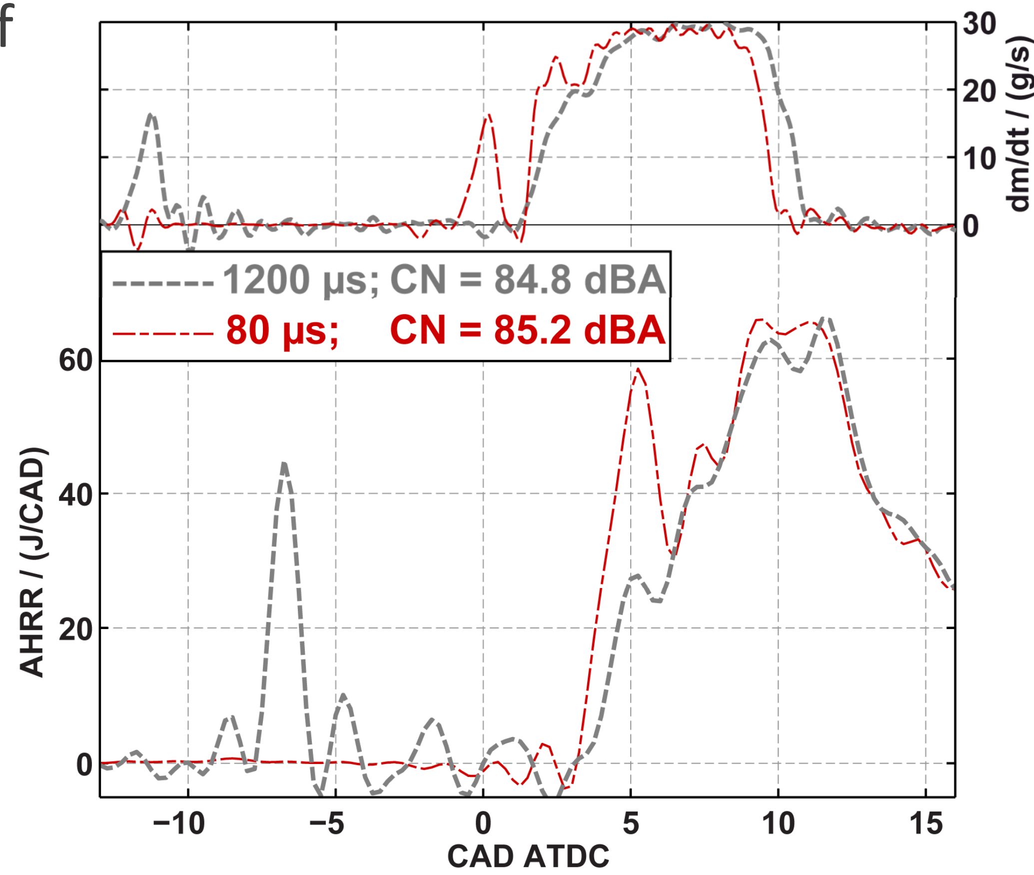

Can main injection rate shaping influence combustion noise?

- Comparison: dwell times of 140 and 500 μs
  - Very similar rates of main injection
  - Dramatic difference in combustion noise
  - Differences in AHRR during main combustion cannot explain the noise difference

- Main injection rate shaping isn't responsible for this combustion noise reduction
  - What else can explain the noise reduction?

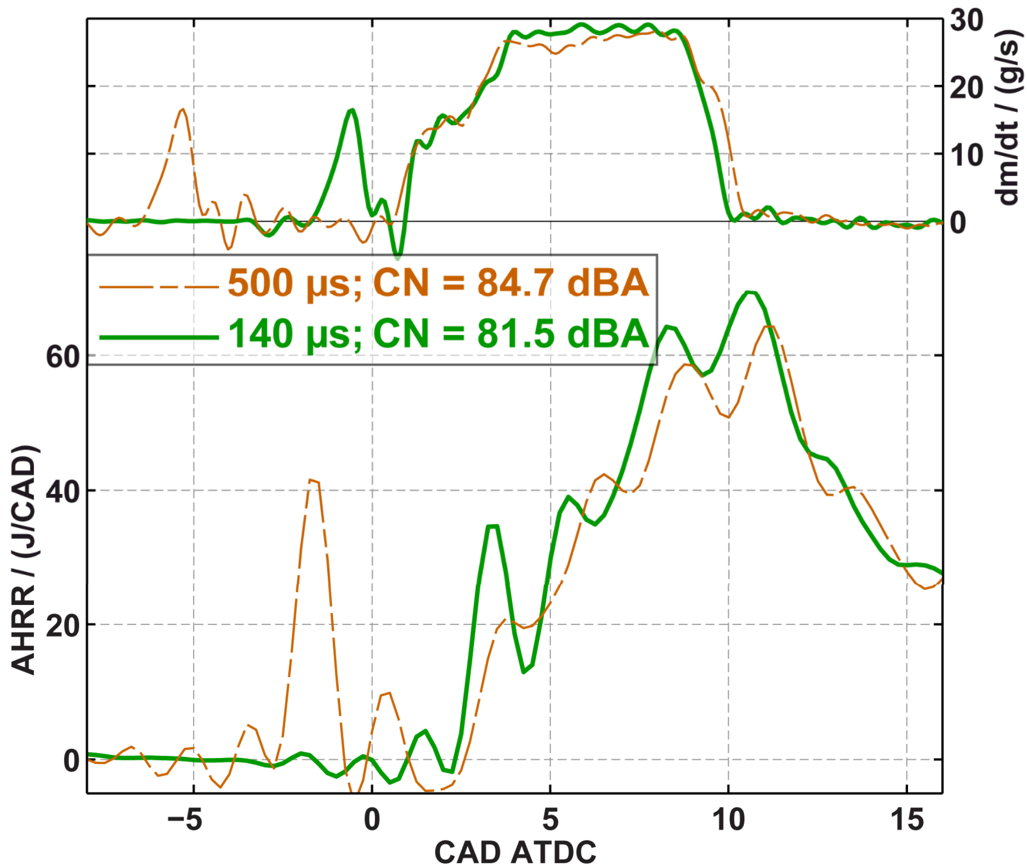

Frequency analysis reveals the spectral range associated with the noise reduction

- Sound pressure level (SPL)
  - Shows each frequency's contribution to audible combustion noise
  - In this case, resonant frequencies contribute little to combustion noise
- Comparison of SPLs from all pilot-main dwells
  - Frequencies most strongly associated with the noise reduction: ~1-3 kHz

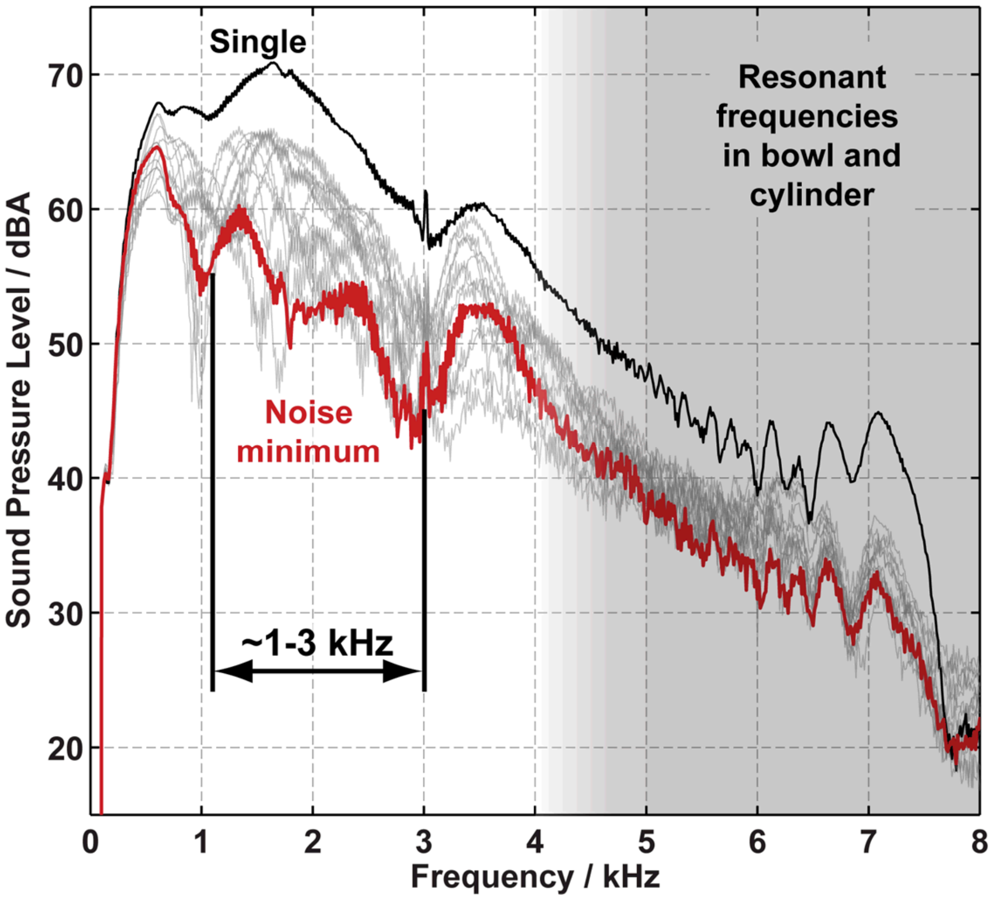

A simple zero-dimensional thermodynamic model to predict combustion noise

- First law of thermodynamics

  $dU = dQ - dW + dm_i h_i - dm_e h_e$

- Idea gas law; continuity

  $PV = mRT;\ dm = dm_i - dm_e$

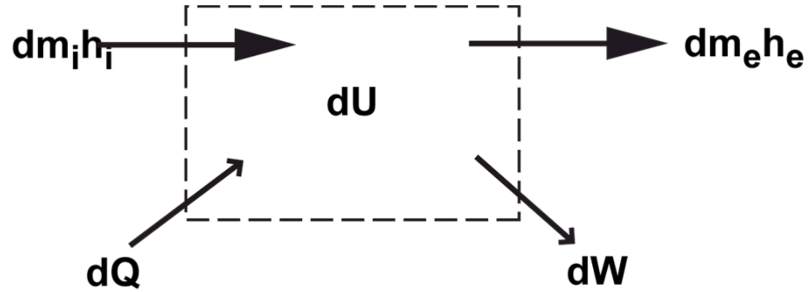

- Differential equations (solved using 4th order Runge-Kutta method):

$$dP = \frac{(\gamma - 1)dQ - \gamma P dV + (\gamma - 1)(dm_i h_i - dm_e h_e)}{V}$$

$$dT = \frac{PdV + VdP}{mR} - T\frac{dm}{m}$$

$$dQ = dQ_{heat\ release} - dQ_{woschni}$$

$$\gamma = 1.35 - 6 \cdot 10^{-5} T + 1 \cdot 10^{-8} T^2$$ (Brunt and Platts, SAE 1999-01-0187)

- Simulation input: heat release profile → $dQ_{heat\ release}$
- Simulation output: cylinder pressure trace, combustion noise

Simulation inputs: pre-defined heat release profiles

- Previous work: combustion noise behavior is well-predicted with realistic heat release profiles
  - SAE 2015-01-0796
- Current work: simplified top hat heat release profiles are used to simplify analyses
  - Total heat release quantities approximate the measured data
  - Combustion dwell: duration between EOC_p and SOC_m
  - Does the close-coupled pilot noise reduction exist with these simple heat release profiles?

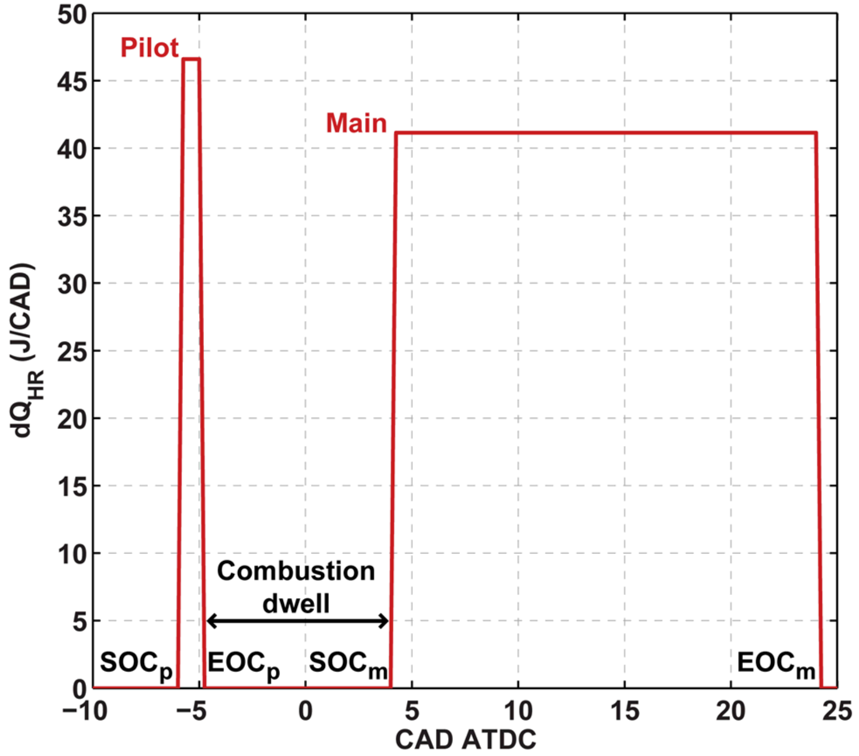

The close-coupled pilot noise reduction occurs with top-hat heat release profiles

- Noise reduction mechanism remains intact
- Details of the noise-dwell curve depend on heat release profile shapes
  - Depth, width of valley, etc.
- What can we learn by digging into the terms of the governing equations?

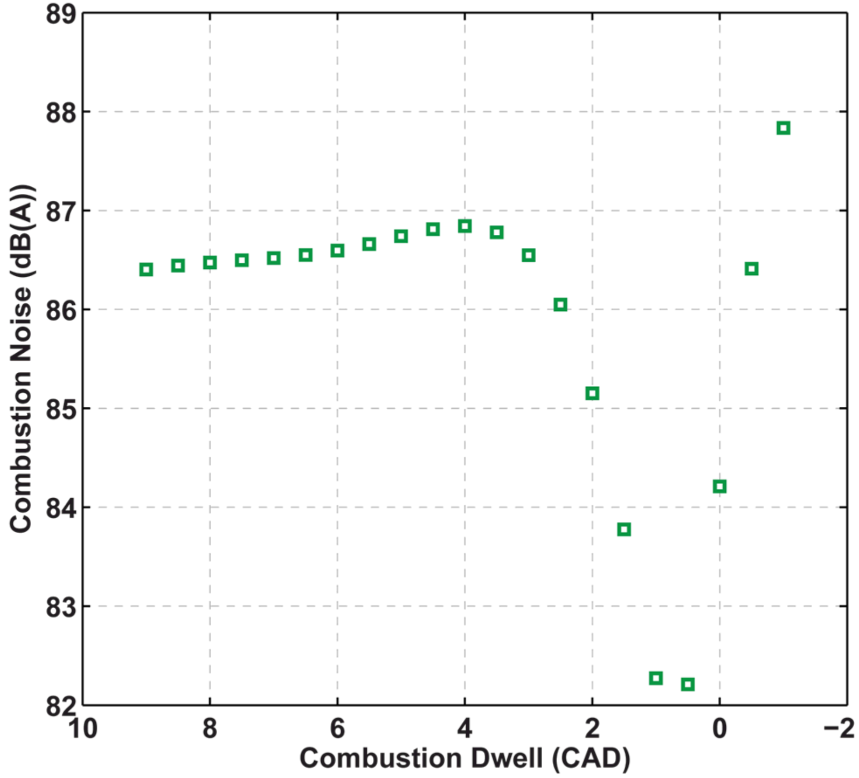

Decomposition of the model's underlying equation for cylinder pressure

$$dP = \frac{(\gamma - 1)(dm_i h_i - dm_e h_e)}{V} + \frac{-\gamma P dV}{V} + \frac{(\gamma - 1)dQ}{V}$$

- $P_{massflow} = \int dP_{massflow}$
  - Not affected by dwell; not responsible for noise reduction
- $P_{work} = \int dP_{work}$
  - Contributes to overall shape of the pressure trace, but not to the noise reduction mechanism
- $P_{heat} = \int dP_{heat}$
  - Changes significantly with dwell; includes wall heat loss and heat release
  - Can be decomposed further

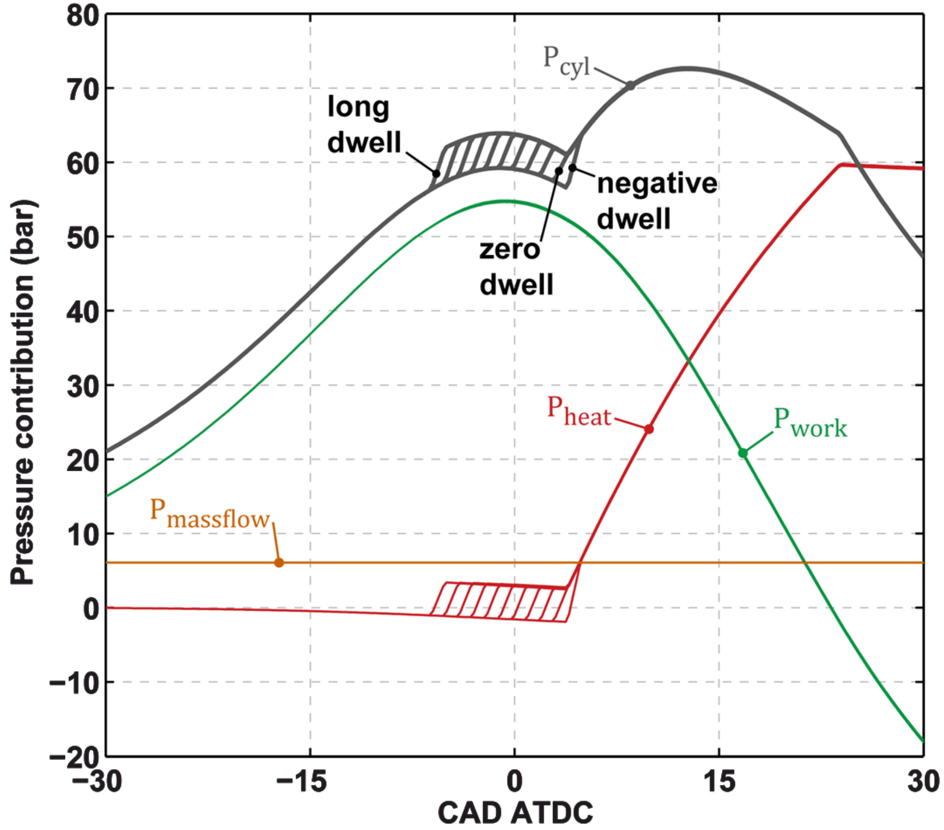

Decomposition of the model's underlying equation for cylinder pressure (cont.)

$$dP_{heat} = \frac{(\gamma-1)dQ_{wall}}{V} + \frac{(\gamma-1)dQ_{HR}}{V}$$

$$P_{wall} = \int \frac{(\gamma-1)}{V} dQ_{wall}$$

- Not affected by dwell; not responsible for noise reduction

$$P_{HR} = \int \frac{(\gamma-1)}{V} dQ_{HR}$$

- This term is fundamentally related to the combustion noise reduction mechanism
- It resembles two superimposed ramped step-functions

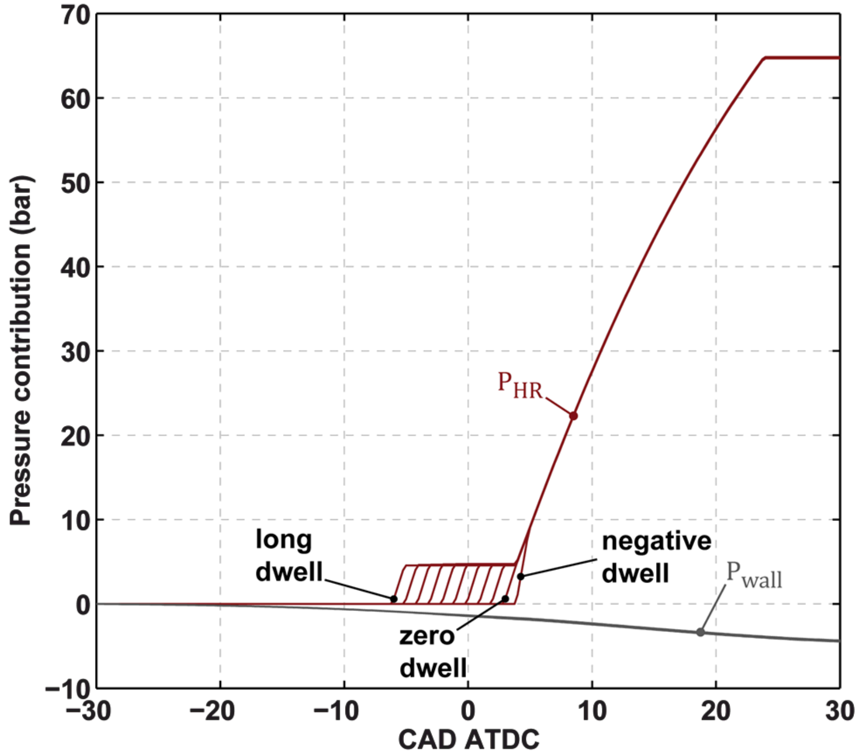

Frequency analysis of simulated cylinder pressure traces

- Simulated SPL spectra do not closely resemble experimentally derived SPL spectra
  - Matching cylinder pressure spectra is not the goal of this work
- A similar frequency band is most closely associated with the noise reduction
  - ~1-3 kHz, depending on details of top-hat heat release profiles
- Approach: band pass filtering of ramped step functions
  - How do ramped steps affect frequency content in the 1-3 kHz range?

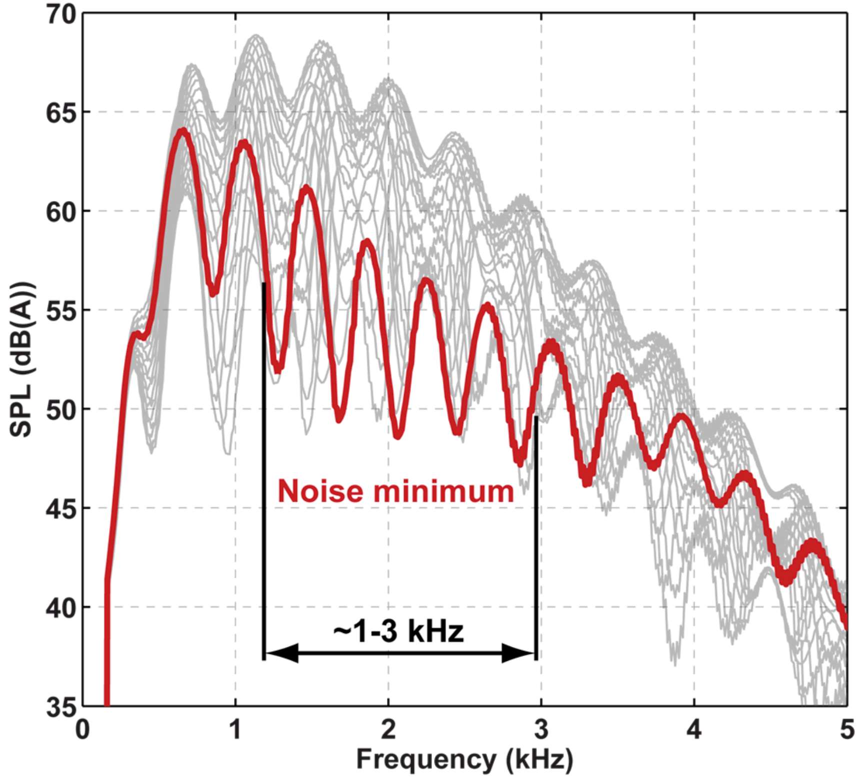

Band pass filtering of a ramp start

- Top: starting portion of a very long pressure ramp of variable slope
- Bottom: band-limited portion of the same pressure ramp
  - Finite impulse response (FIR) band pass filter: 1-3 kHz
- An abrupt increase in slope produces strong band-limited oscillations near the “corner”
  - A larger slope means higher band-limited oscillation amplitudes
- What about the end of a pressure ramp?

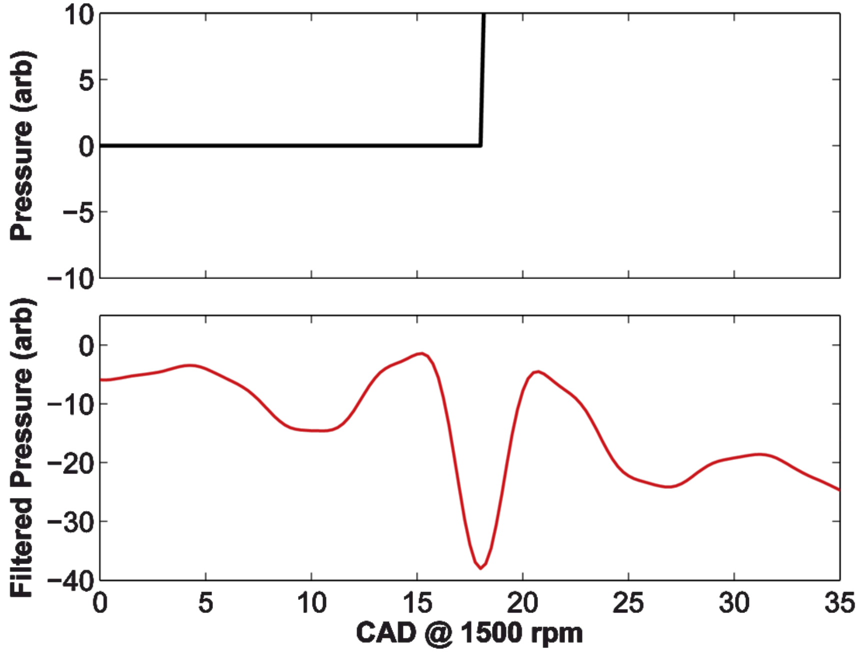

Band pass filtering of the start and end of a positive ramp

- Pressure oscillations at the end of a positive ramp (top) are an inverted image of the oscillations at the start of the ramp (bottom)
- Every ramped step is a combination of these two features
  - Pilot: ramp start followed closely by ramp end
  - Main: ramp start, long ramp, followed by ramp end

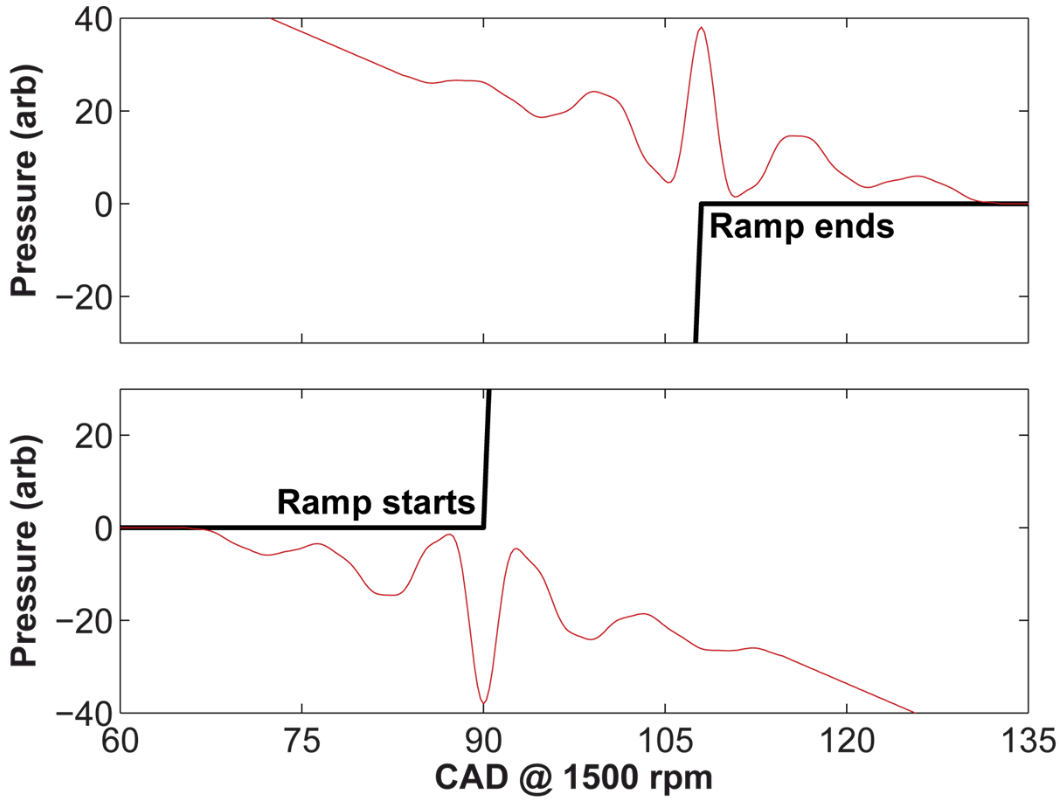

Combustion noise reduction through destructive interference

- Band-limited pilot ramp: trough followed by peak
- Band-limited main ramp: two peaks surrounding a trough
- Superposition of these two band-limited pressure traces with variable phasing
- Frequency content in 1-3 kHz band is attenuated through destructive interference
- **This is the heart of the close-coupled pilot combustion noise reduction mechanism!**

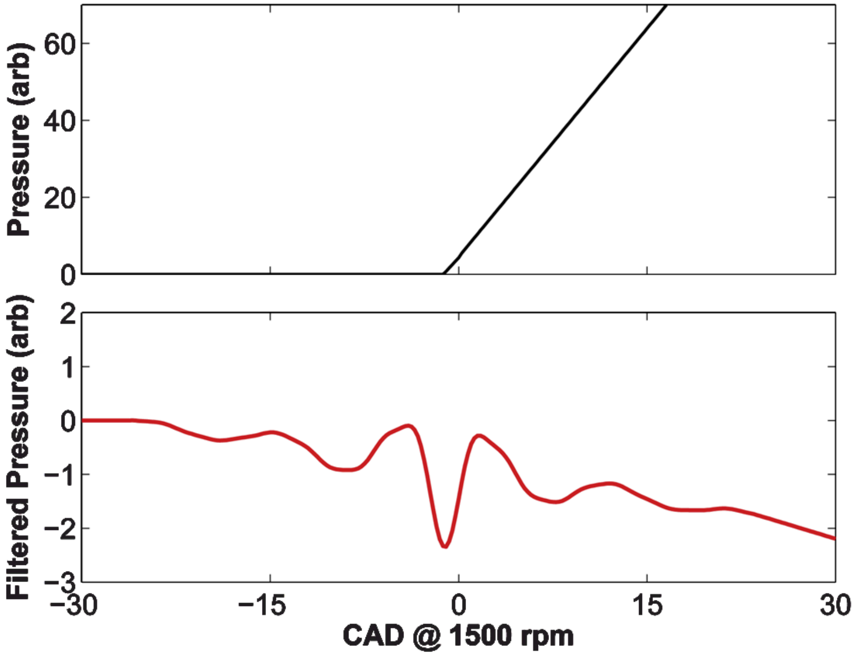

Recap: combustion noise reduction with close-coupled pilot injections

- $P_{HR} = \int \frac{(\gamma - 1)}{V} dQ_{HR}$
  - The rate of pressure rise due to heat release is directly proportional to the heat release rate
  - A constant heat release rate results in a nearly constant pressure rise rate – a pressure ramp
- The starts and ends of pressure ramps are associated with significant frequency content (visualized with bandpass filtered pressure oscillations)
- The frequency components in the 1-3 kHz range of a pressure ramp form waveforms with the potential to interact with other pressure ramps
- With the superposition of properly shaped and phased pressure ramps, destructive interference of the higher frequency components is possible
- Does this apply to measured cylinder pressure data?

Evidence of destructive interference with close-coupled pilots: experimental data

- Band-limited pilot ramp: trough followed by peak
- Band-limited main ramp: two peaks surrounding a trough
- Dwell decreases; pilot and main oscillations begin to interact
- Minimum combustion noise: destructive interference of pilot and main oscillations is maximized
- **Destructive interference of higher frequency components (1-3 kHz in this case) can reduce combustion noise in an engine!**

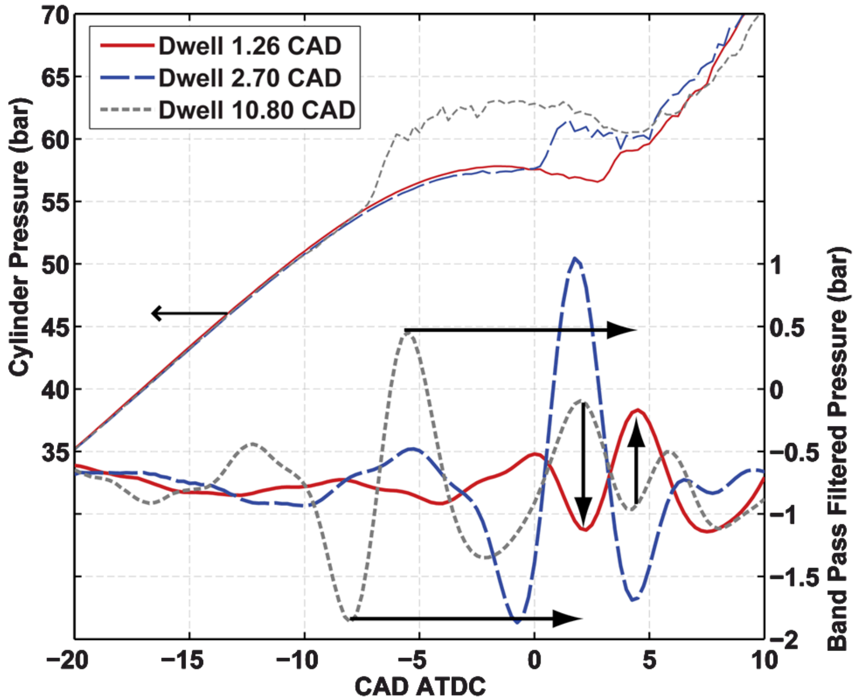

Impact of combustion phasing on close-coupled pilot noise reduction

- The combustion noise reduction occurs regardless of overall combustion phasing
- The combustion dwell for minimum noise does not depend on combustion phasing

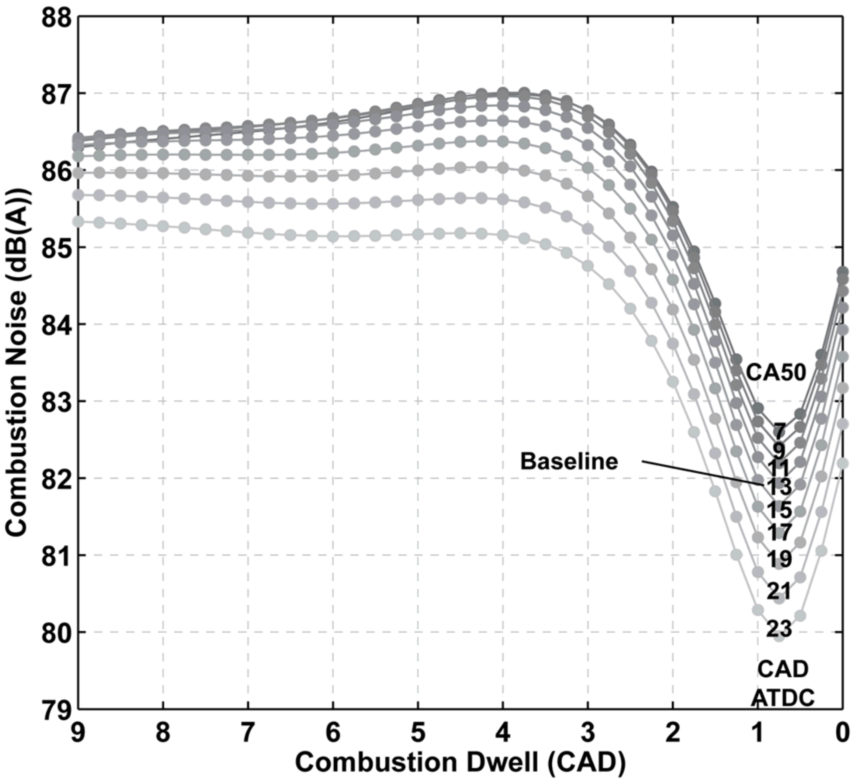

Does peak pressure rise rate correlate with combustion noise?

- If the close-coupled pilot noise reduction mechanism is active, $dP/d\theta_{max}$ is not a reliable indicator of combustion noise
- Close-coupled pilots may be much more effective than retarding combustion phasing to reduce noise
  - This could enable efficiency benefits for noise-limited operating points

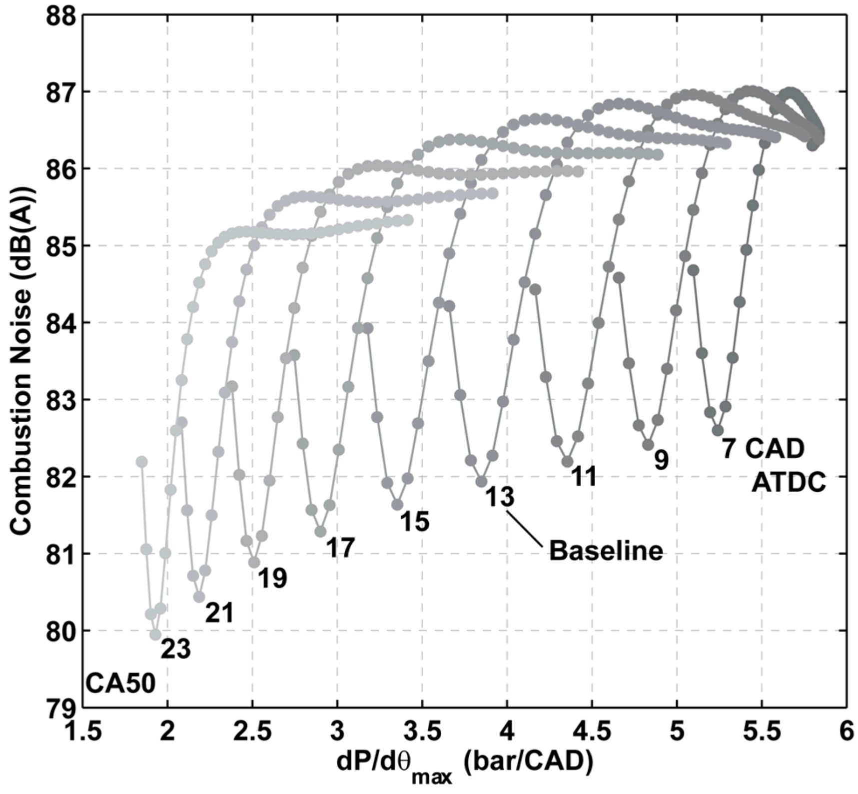

Impact of main heat release rate profile on combustion noise

- Three different dwells, variation of main heat release rise rate
  - Peak main heat release rate and total heat released held constant
- Far/intermediate pilots: increasing main heat release ramp rate increases noise
- Close-coupled pilots: increasing main heat release ramp rate can decrease noise!
- Decreasing the main heat release ramp rate degrades its potential for noise reduction

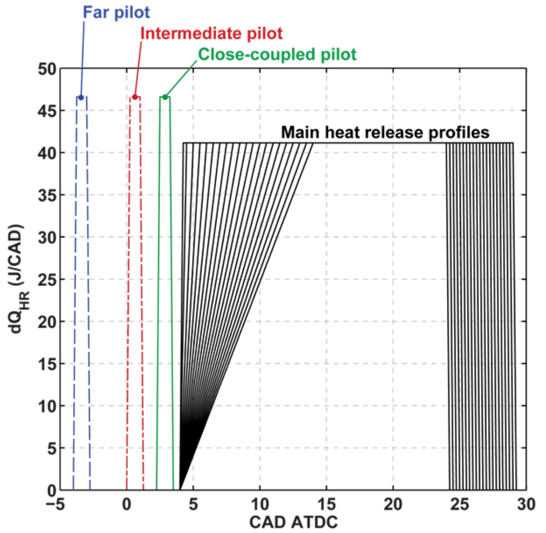

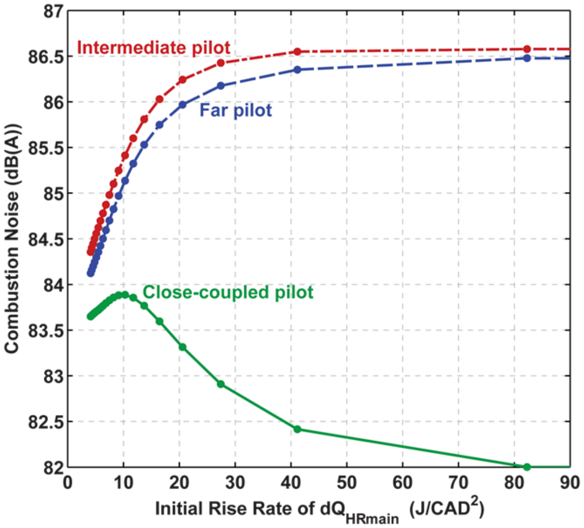

Impact of main heat release rate profile on combustion noise (cont.)

- The shape of the early main heat release impacts the relationship between combustion noise and dwell
- More robust main heat release increases noise for far pilots, but increases the noise reduction potential
- The sensitivity of noise to dwell increases as the early main heat release intensifies
  - Possible tradeoff between noise reduction potential and robustness

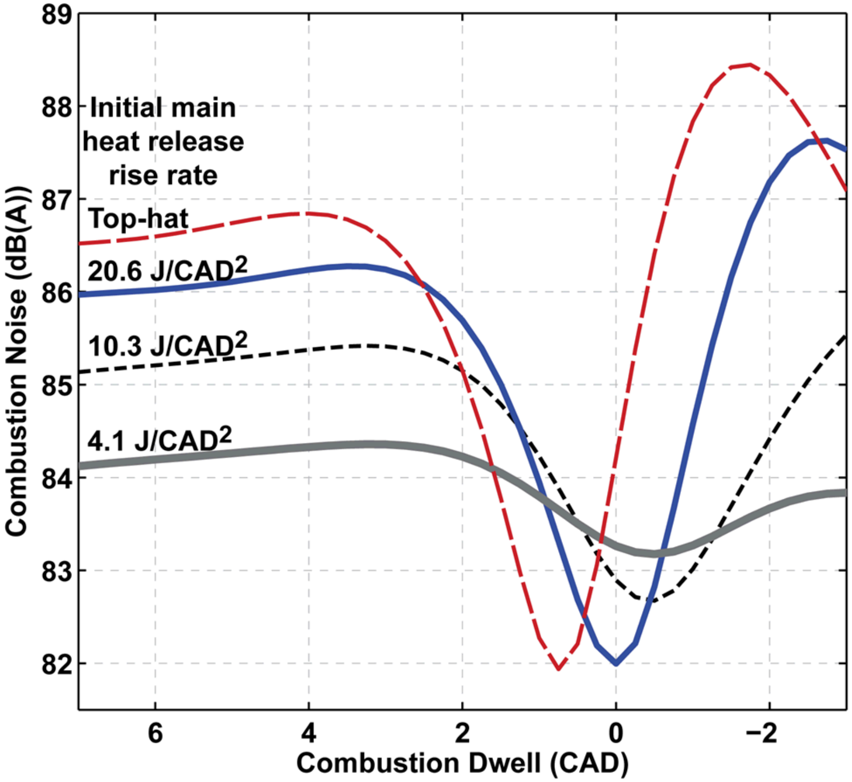

Summary / Conclusions

- Zero-dimensional thermodynamic model provides a theoretical basis for combustion noise reduction by close-coupled pilots
- Combustion noise reduction mechanism:

FREquency Band interference for the Attenuation of COmbustion Noise

FREBACON

  - Shapes and phasing of pilot and main heat release events matter

- This mechanism can potentially improve noise-efficiency tradeoffs, but has not yet been demonstrated over a wide range of conditions
- Can this noise reduction mechanism be applied to advanced compression ignition combustion strategies in which excessive noise is a problem?

THANK YOU FOR YOUR ATTENTION!

Questions?

For more detail, please see:

Busch, S., Zha, K., Warey, A., Pesce, F. C. and Peterson, R., "On the Reduction of Combustion Noise by a Close-Coupled Pilot Injection in a Small-Bore Direct Injection Diesel Engine," J. Eng. Gas Turbines Power 138(10), 102804 (Apr 12, 2016) (13 pages) Paper No: GTP-16-1041; doi: 10.1115/1.4032864

Impact of pilot quantity on combustion noise reduction potential

- Scale pilot heat release rate by a constant factor (increase pressure ramp rate for constant duration)
- Increasing pilot quantity increases combustion noise, but the noise reduction potential may decrease for higher quantities
- Destructive interference is most effective when both waveforms are of similar magnitude
- Too much pilot fuel degrades the potential for destructive interference

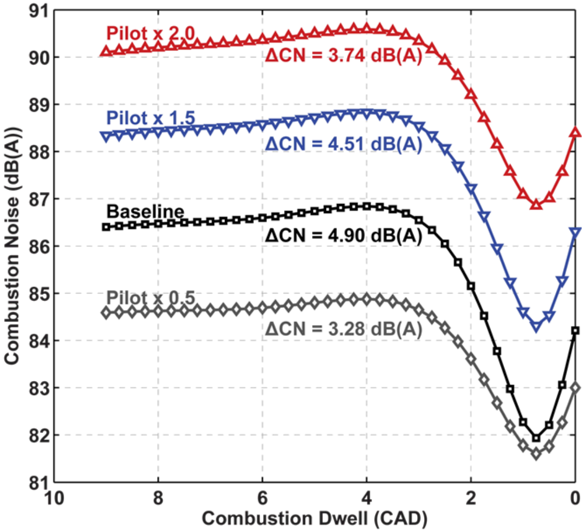

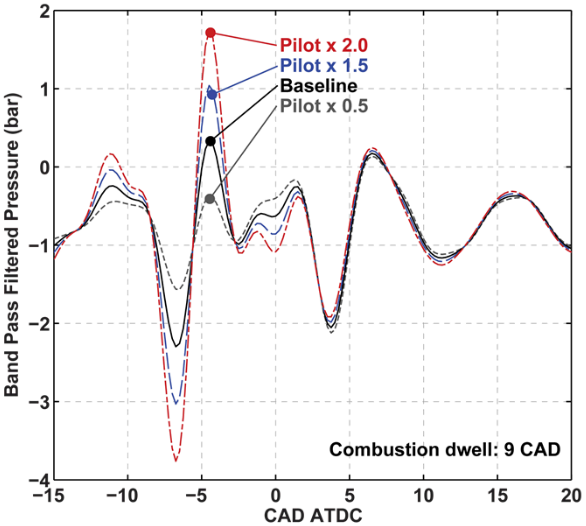

Simulation of gas exchange process

- Compressible flow though valves (from Heywood, 1988)
  - Choked flow

$$\text{if } \frac{P_{low}}{P_{hi}} \leq \left(\frac{2}{\gamma-1}\right)^{\gamma/\gamma-1}$$

$$\dot{m} = \frac{C_D A_R P_{hi}}{\sqrt{RT_0}} \sqrt{\gamma} \left(\frac{2}{\gamma+1}\right)^{(\gamma+1)/2(\gamma-1)}$$

  - Non-choked flow

$$\dot{m} = \frac{C_D A_R P_{hi}}{\sqrt{RT_0}} \left(\frac{P_{low}}{P_{hi}}\right)^{1/\gamma} \sqrt{\frac{2\gamma}{\gamma-1}\left[1-\left(\frac{P_{low}}{P_{hi}}\right)^{\gamma-1/\gamma}\right]}$$

- Valve lift and valve flow coefficient data have been measured
- Intake and exhaust pressures assumed to be constant
- Not as accurate as measured cylinder pressure during gas exchange, but adequate for a simple model

Can maximum rate of pressure rise be used to predict combustion noise trends?

- Maximum rate of pressure rise for filtered cylinder pressure
- Trend in $dP/d\theta_{max}$ does not reflect the noise behavior for short dwell times

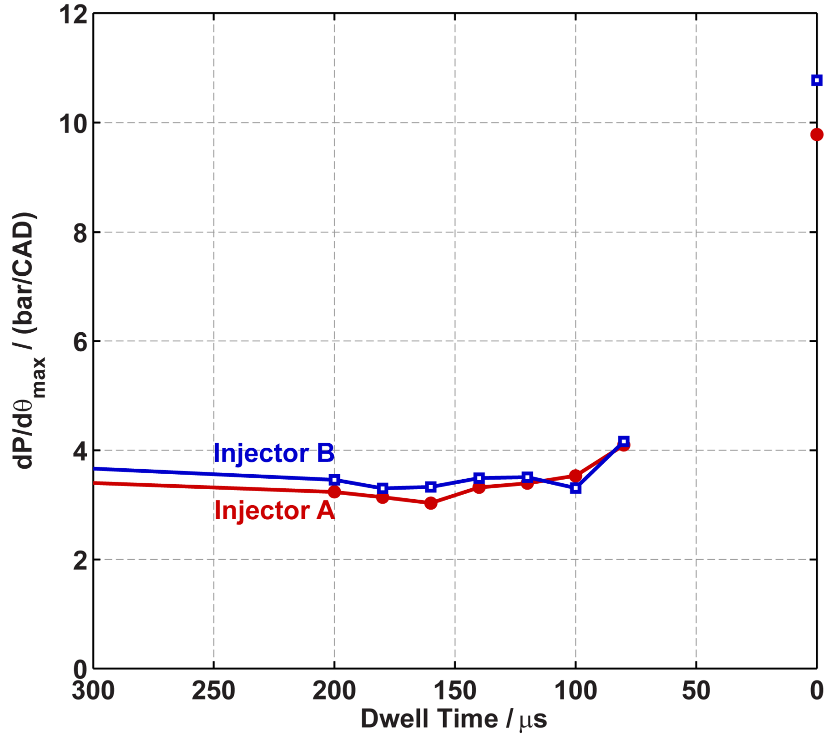

Model validation

- Reasonable agreement with experimental data
- Pilot heat release appears to be well-modeled as a rectangular profile
- Main heat release profile deviates from a rectangle
  - Motivation for main heat release ramp variation

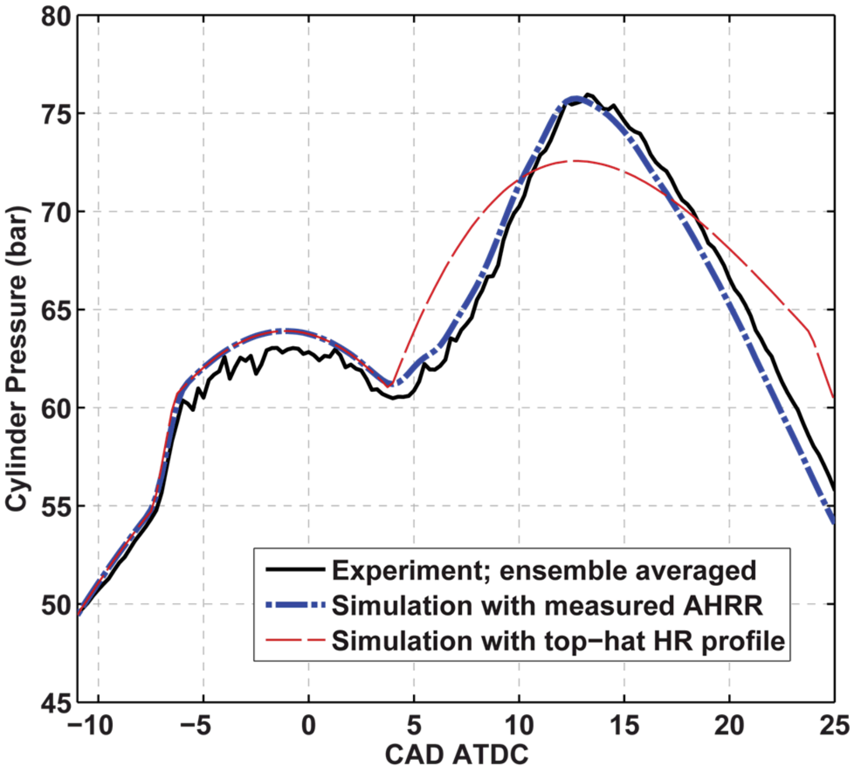

Ramp slope variation (long ramp)

- The effect of heat-release on cylinder pressure:
  - $dP = \frac{(\gamma-1)dQ}{V} + \cdots$
- The contribution of a heat-release event of finite duration to the cylinder pressure trace can be approximated by a ramped step
- As the ramp becomes steeper, the harmonics associated with it become more intense
- As the duration of the ramp changes, the shape of the band-limited pressure trace changes
- The combination of ramp shape and duration determines noise reduction potential

Constant ΔP, variable slope (dQ) and duration

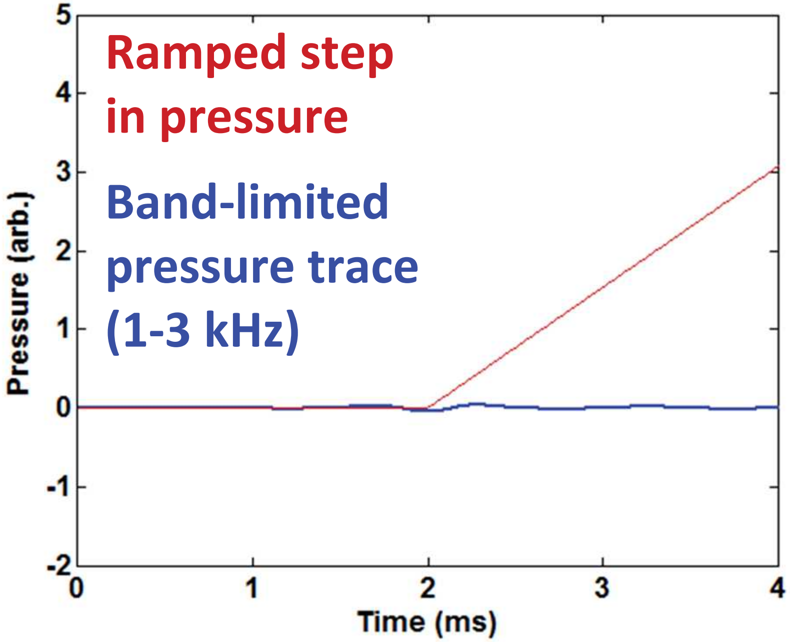

Ramp duration variation (constant slope)

- The effect of heat-release on cylinder pressure:
  - $dP = \frac{(\gamma - 1)dQ}{V} + \cdots$
- The contribution of a heat-release event of finite duration to the cylinder pressure trace can be approximated by a ramped step
- For a given ramp slope, the duration of the heat release event strongly affects the frequency content
- The start and end of heat release have a distinctive band-limited pressure signature

Constant slope (dQ), variable duration

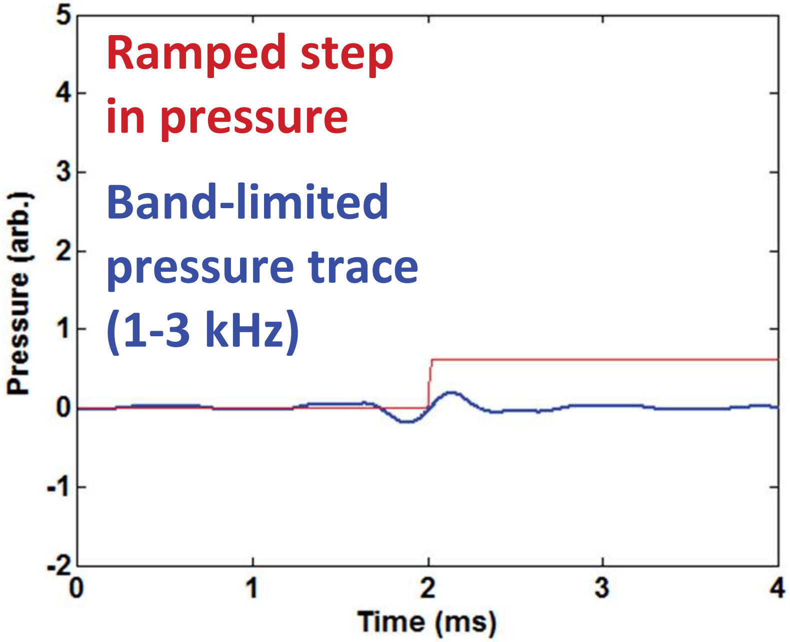

Ramp slope variation (constant duration)

- The effect of heat-release on cylinder pressure:
  - $dP = \frac{(\gamma - 1)dQ}{V} + \cdots$
- The contribution of a heat-release event of finite duration to the cylinder pressure trace can be approximated by a ramped step
- For a given duration, the band-limited pressure signature increases in amplitude as slope increases

Constant duration, variable slope (dQ)